SEARCHING FOR QCD INSTANTONS VIA TAGGING FORWARD PROTONS*

Marek Taševský

Institute of Physics of the Czech Academy of Sciences
Na Slovance 2, Prague, 18221, Czech Republic
Marek.Tasevsky@cern.ch

Received 3 June 2025, accepted 11 October 2025, published online 19 December 2025

Although the QCD instanton has been intensively searched for in several experiments, it has not yet been observed. Here, we study the possibility of observing heavy ($M_{\rm inst} > 60$ GeV) QCD instantons at the LHC in the diffraction mode, *i.e.* in events with one or two tagged leading protons which are accompanied by large rapidity gaps. The presented analysis provides a detailed look into the experimental situation and accounts for detector and pile-up effects. We show that the expected instanton signal in a single-tagged configuration is strongly affected by central detector and pile-up effects but observable. For the double-tagged approach, the combinatorial background overwhelms the expected signal. Possible improvements lie in adding time information about tracks at central and forward rapidities.

DOI:10.5506/APhysPolBSupp.18.6-A28

1. Introduction

This text only describes the main points of the analysis which has been published in Ref. [1] where all details and references can be found.

Instantons are non-perturbative classical solutions of Euclidean equations of motion in non-Abelian gauge theories [2]. In the semi-classical limit, instantons describe quantum tunneling between different vacuum sectors of the theory [3–5]. Up to now, the QCD instanton has never been observed experimentally. The problem is that the large-size instanton is very challenging to distinguish from various possible soft QCD contributions, while the cross section of the heavy (small-size) instanton production is exponentially suppressed by the e^{-2S_I} factor, where the corresponding to instanton action is $S_I = 2\pi/\alpha_{\rm s}$. On the other hand, in the case of the small-size instanton signal, the uncertainties due to the soft QCD and other non-perturbative

* Presented at the V4-HEP 3 — Theory and Experiment in High Energy Physics Workshop, Prague, Czech Republic, 1–4 October, 2024.

effects are under better control. The characteristic signature of a small-size instanton is the production of a large number of isotropically distributed (mini)jets. That is, we are searching for the high multiplicity events with large (close to 1) sphericity S. However, it was shown in Ref. [6] that at high multiplicities, the role of the multiple parton interactions (MPI) strongly increases and the resulting sphericity of these MPI events also becomes close to unity. Therefore, first of all, we have to suppress the MPI contributions. This can be done by selecting the events with large rapidity gaps (LRGs), as demonstrated in Ref. [7].

While the QCD instanton production in inclusive events at the LHC was considered in Refs. [8–10], Ref. [1] elaborates on the possibility of observing the higher-mass instantons ($M_{\rm inst} > 60$ GeV) in the diffraction mode, *i.e.* by tagging the leading protons with the dedicated forward proton detectors (FPDs): AFP [11, 12] on the ATLAS side or CT-PPS [13, 14] on the CMS side, when the remaining fraction of beam energy is $\xi = 1 - x_{\rm L} \sim 0.03$. Due to the strong $\mathrm{e}^{-2\pi/\alpha_{\rm s}}$ suppression of a heavy instanton amplitude, the expected cross section becomes rather small. Thus, we have to consider the possibility of working at a large luminosity and account for the pile-up effects. We study the 'one LRG' kinematics, where only one leading proton is detected as well as the central instanton production, when both leading protons are observed, see Fig. 1. If the instanton is produced by a two-gluon initial state, the final state of this instanton-mediated process will have N_f pairs of quarks and anti-quarks with the same chirality

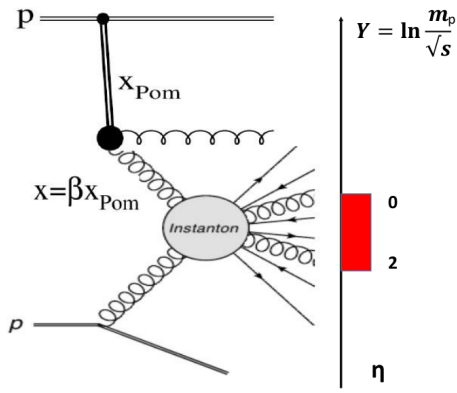

Fig. 1. Instanton production in a diffractive process with an LRG. The Pomeron exchange is shown by the thick doubled line. The red bar shows the range of η considered in Ref. [1]. Y indicates the incoming proton position in rapidity. As shown in the diagram secondaries will be also produced outside this range but they will not be used when calculating $E_{\rm T}$ or $N_{\rm ch}$.

$$g + g \to n_g \times g + \sum_{f=1}^{N_f} (q_{Rf} + \bar{q}_{Lf}) \ , \tag{1}$$

where N_f is the number of light flavours relative to the inverse instanton size, $m_f < 1/\rho$. Thus, to discover the QCD instanton, we have to observe in the final state a multi-particle cluster or a fireball which contains, in general, a large number of isotropically distributed gluon (mini)jets accompanied by N_f pairs of light quark jets generated by a subprocess such as in Eq. (1).

2. The analysis procedure

The analysis described in Ref. [1] extends all previous LHC-oriented theory or phenomenology studies by including the following three steps which are all time (and space)-consuming: *(i)* MPI (using PYTHIA 8.2 [15]), *(ii)* detector effects, and *(iii)* pile-up effects (both using Delphes 3.5 [16]). The results are presented in the form of numbers of expected events at the detector level for four luminosity scenarios. This way, we believe, one can rather easily judge the feasibility of the proposed measurement. The effect of pile-up manifests itself at two levels: in the central detector (where it can smear cluster energies or track properties using actual subdetector resolutions) and in FPDs, where it gives rise to combinatorial background. The latter is caused by a combination of two or three independent events (all coming from the same bunch crossing) which may mimic the signal perfectly. This type of background can be reduced by making use of the time-of-flight detector, see *e.g.* the detector paper from Run 2 [17] and the phenomenology studies in Ref. [18].

2.1. MC samples and selection cuts

In this study, we work at $\sqrt{s} = 14$ TeV and we scrutinize two mass regions, namely $M_{\rm inst} > 60$ GeV and $M_{\rm inst} > 100$ GeV, both in the FPD acceptance $0.02 < \xi < 0.05$ and for the single-tagged (ST) configuration, the latter also for the double-tagged (DT) configuration. In total, we then work with three instanton signal event samples. All are generated using the RAMBO algorithm [19] at $\xi = 0.03$, with proton–Pomeron collision type for the ST approach (2.5×10^6 events for $M_{\rm inst} > 60$ GeV and 5×10^5 events for $M_{\rm inst} > 100$ GeV) and with Pomeron–Pomeron collision type for the DT approach (10^5 events). The respective instanton production cross sections integrated over the $0.02 < \xi < 0.05$ region are 1004.6 pb and 39.6 pb for the proton–Pomeron sample and for $M_{\rm inst} > 60$ GeV and 100 GeV, respectively, and 500 fb for the Pomeron–Pomeron sample and $M_{\rm inst} > 100$ GeV. All samples are showered and hadronised using PYTHIA 8.2 with initial-state radiation (ISR), final-state radiation (FSR), and the MPI switched on.

For simplicity, in all cases, the instanton signal is generated with a forward leading proton only in one hemisphere with $p_z < 0$. For this reason, in the following, all studies are done and all cuts are tailored for one hemisphere. Assuming a full symmetry in z coordinate, the final numbers are then obtained by doubling those from the studied hemisphere.

For both, ST and DT approaches, we consider two combinatorial backgrounds, one based on the dijet production in single-diffractive (SD), the other on dijets in non-diffractive (ND) interactions, which are by far most dominant due to the resemblance of their final states to the final state of the signal and due to their huge production cross sections with respect to that of the signal. In both, again ISR, FSR, and MPI are switched on. For the SD dijet background, we use the dynamical gap survival approach with MPI between Pomeron and proton switched on [20]. Production cross sections for $\hat{p}_{\mathrm{T,min}} > 10$ GeV are 80 μb for SD and 8.64 mb for ND. At the truth level, we have generated roughly 5×10^{11} SD events and 8.5×10^{11} ND events. Subsamples of these as well as all signal samples were simulated using Delphes 3.5.

After examining nearly 50 cut scenarios including all the effects from steps *(i)–(iii)* listed above, the following set of cuts has been found to give the best signal-to-background (S/B) ratio at the detector level Eq. (2) for $M_{\mathrm{inst}} > 60$ GeV and Eq. (3) for $M_{\mathrm{inst}} > 100$ GeV

$$N_{\mathrm{tr05}} > 25 \text{ and } N_{\mathrm{tr20}} = 0 \text{ and } \sum E_{\mathrm{T}}^{\mathrm{fwcalo}} < 5 \text{ GeV and } \xi^{\mathrm{calo}} < 0.025\,, \quad (2)$$

$$N_{\mathrm{tr05}} > 30 \text{ and } N_{\mathrm{tr25}} = 0 \text{ and } \sum E_{\mathrm{T}}^{\mathrm{fwcalo}} < 5 \text{ GeV and } \xi^{\mathrm{calo}} < 0.025\,, \quad (3)$$

where N_{tr05}, N_{tr25}, and N_{tr20} are numbers of tracks in the $0.0 < \eta < 2.0$ region and for $p_{\mathrm{T}} > 0.5$ GeV, $p_{\mathrm{T}} > 2.5$ GeV, and $p_{\mathrm{T}} > 2.0$ GeV, respectively, and $E_{\mathrm{T}}^{\mathrm{fwcalo}}$ is a sum of E_{T} of clusters in the forward calorimeter with $p_{\mathrm{T}} > 0.5$ GeV and $2.5 < \eta < 4.9$. The ξ^{calo} quantity is calculated as a sum of $E_{\mathrm{T}}\,\mathrm{e}^{-\eta}$ over calorimeter clusters with $E_{\mathrm{T}} > 0.2$ GeV.

3. Results

3.1. Single tag

To illustrate the situation after data taking at the detector level, the expected event yields for signal generated with $M_{\mathrm{inst}} > 60$ GeV and $M_{\mathrm{inst}} > 100$ GeV together with the combinatorial backgrounds, from both the SD dijets and ND dijets, are shown in Figs. 2 and 3 as functions of S_{T} for four luminosity scenarios, after applying detector-level cuts defined in Eq. (2) and Eq. (3), respectively.

The final event yields for signal, combinatorial SD and ND dijet backgrounds are shown in Table 1.

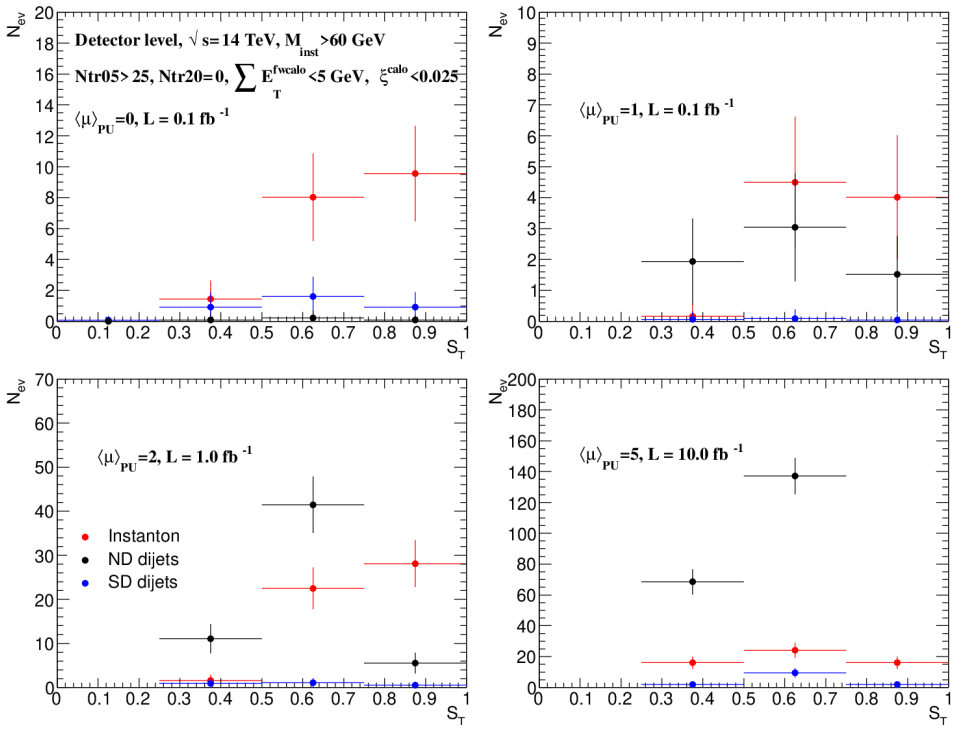

Fig. 2. Distributions of expected event yields as functions of transverse sphericity at the detector level for the instanton signal from proton–Pomeron collisions generated by RAMBO for $M_{\text{inst}} > 60$ GeV and the combinatorial backgrounds from ND dijets and SD dijets generated by PYTHIA 8.2 after applying detector-level cuts in Eq. (2) for four luminosity scenarios. Only statistical uncertainties are shown, estimated using expected event numbers from Table 1.

Table 1. Summary of event yields after applying cuts in Eq. (2) and Eq. (3) for the single-tag search approach for $M_{\text{inst}} > 60$ GeV and $M_{\text{inst}} > 100$ GeV, respectively, and for four luminosity scenarios ($\langle\mu\rangle$, $\mathcal{L}$). For each scenario, a ratio of the number of signal to combinatorial background events, $N_{\text{S}}/(N_{\text{ND}} + N_{\text{SD}})$, is shown.

$(\langle\mu\rangle, \mathcal{L}\ [\text{fb}^{-1}])$	$M_{\text{inst}} > 60$ GeV	$M_{\text{inst}} > 100$ GeV
(0, 0.1)	19.0/(0.4+3.5)	5.8/(0.2+3.5)
(1.0, 0.1)	8.7/(6.5+0.2)	3.2/(4.7+0.2)
(2.0, 1.0)	52.2/(58.1+2.5)	15.4/(55.3+2.2)
(5.0, 10.0)	56.2/(205.6+13.3)	23.8/(137.1+7.6)

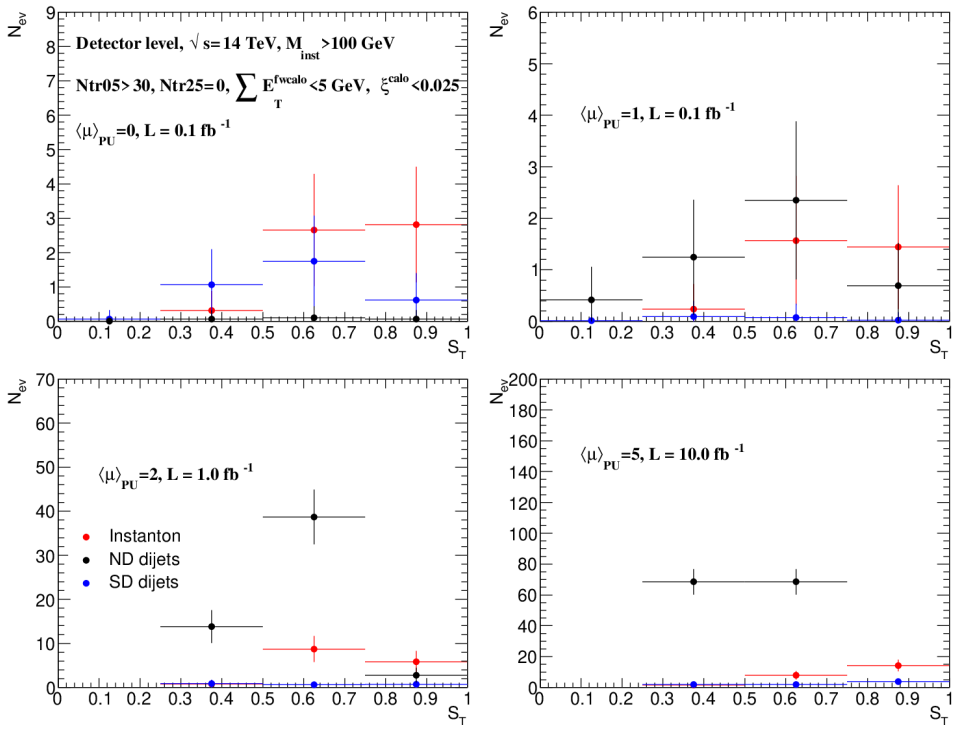

Fig. 3. Distributions of expected event yields as functions of transverse sphericity at the detector level for the instanton signal from proton–Pomeron collisions generated by RAMBO for $M_{\mathrm{inst}} > 100$ GeV and the combinatorial backgrounds from ND dijets and SD dijets generated by PYTHIA 8.2 after applying detector-level cuts in Eq. (3) for four luminosity scenarios. Only statistical uncertainties are shown, estimated using expected event numbers from Table 1.

For the specific cut scenarios in Eq. (2) and Eq. (3) considered for the two mass intervals, we observe that the S/B ratio safely exceeds unity when pile-up is not considered, thanks to the efficient ξ^{calo} cut. If we require $\xi^{\mathrm{calo}} < 0.025$, the S/B stays above unity for $\langle\mu\rangle = 1$ and $M_{\mathrm{inst}} > 60$ GeV, all other luminosity scenarios give S/B below 1.0. Its value further decreases with increasing $\langle\mu\rangle$ and reaches minima of 0.3 (0.2) at $\langle\mu\rangle = 5$ for $M_{\mathrm{inst}} > 60$ (100) GeV. It is therefore a clear preference to collect data at rather low amounts of pile-up, and we believe that a special run with $\langle\mu\rangle \sim 1$ and $\mathcal{L} \sim 0.1$ fb^{-1} is realistic to consider.

3.2. Double tag

The advantages of the double-tagged approach are manifold. For the Pomeron–Pomeron case, the colliding energy is relatively low, which strongly reduces the multiplicity of the background underlying events. Furthermore, detecting two outgoing protons would allow one to place an upper limit on the instanton mass. However, since the production cross section is by a factor of 80 lower than in the ST case, we have to consider higher integrated luminosities, hence higher instantaneous luminosities which entail significant pile-up effects, despite the very narrow ξ range chosen. For two luminosity scenarios, now with significantly more pile-up, namely $(\langle\mu\rangle,\ \mathcal{L}\ [\mathrm{fb}^{-1}]) = (20, 60)$ and (50, 300), the S/B ratio would drop by a factor of 16 and by two orders of magnitude, respectively, when compared with the S/B ratio for the luminosity scenario (1, 0.1) in the ST approach, even after including the suppression of this background thanks to the ToF detector (which is available for double-tagged events).

4. Summary

The effects of MPI, detector acceptance, and resolution, and of pile-up are strong in the case of searching for the QCD instanton in the diffraction mode. To keep the combinatorial background at a tolerable level, the instantaneous luminosity has to be kept low which, together with a limited time to collect the data, leads to modest signal event yields. With a carefully chosen set of cuts and keeping also values of the ξ variable relatively low, the signal-to-background ratio is expected to exceed unity in the mode with one tagged forward proton. The timing information from the central and forward detectors would help to suppress the combinatorial background further.

REFERENCES

[1] M. Tasevsky, V. Khoze, D. Milne, M. Ryskin, *Eur. Phys. J. C* **83**, 35 (2023), arXiv:2208.14089 [hep-ph].

[2] A.A. Belavin, A.M. Polyakov, A.S. Schwartz, Y.S. Tyupkin, *Phys. Lett. B* **59**, 85 (1975).

[3] G. 't Hooft, *Phys. Rev. D* **14**, 3432 (1976).

[4] C.G. Callan, Jr., R.F. Dashen, D.J. Gross, *Phys. Lett. B* **63**, 334 (1976).

[5] R. Jackiw, C. Rebbi, *Phys. Rev. Lett.* **37**, 172 (1976).

[6] M. Sas, J. Schoppink, *Nucl. Phys. A* **1011**, 122195 (2021), arXiv:2101.12367 [hep-ph].

[7] V.A. Khoze, V.V. Khoze, D.L. Milne, M.G. Ryskin, *Phys. Rev. D* **104**, 054013 (2021), arXiv:2104.01861 [hep-ph].

[8] V.V. Khoze, F. Krauss, M. Schott, *J. High Energy Phys.* **2020**, 201 (2020), arXiv:1911.09726 [hep-ph].

[9] V.V. Khoze, D.L. Milne, M. Spannowsky, *Phys. Rev. D* **103**, 014017 (2021), arXiv:2010.02287 [hep-ph].

[10] S. Amoroso, D. Kar, M. Schott, *Eur. Phys. J. C* **81**, 624 (2021), arXiv:2012.09120 [hep-ph].

[11] ATLAS Collaboration (L. Adamczyk *et al.*), «Technical Design Report for the ATLAS Forward Proton Detector», CERN-LHCC-2015-009; ATLAS-TDR-024.

[12] ATLAS Collaboration (M. Tasevsky), *AIP Conf. Proc.* **1654**, 090001 (2015).

[13] M. Albrow *et al.*, «CMS-TOTEM Precision Proton Spectrometer», Tech. Rep. CERN-LHCC-2014-021. TOTEM-TDR-003. CMS-TDR-13, CERN, Geneva, Sep. 2014.

[14] CMS Collaboration (M. Albrow *et al.*), arXiv:2103.02752 [physics.ins-det].

[15] T. Sjöstrand *et al.*, *Comput. Phys. Commun.* **191**, 159 (2015), arXiv:1410.3012 [hep-ph].

[16] DELPHES 3 Collaboration (J. de Favereau *et al.*), *J. High Energy Phys.* **2014**, 057 (2014), arXiv:1307.6346 [hep-ex].

[17] ATLAS Collaboration (G. Aad *et al.*), *J. Instrum.* **19**, P05054 (2024), arXiv:2402.06438 [physics.ins-det].

[18] K. Černý, T. Sýkora, M. Taševský, R. Žlebčík, *J. Instrum.* **16**, P01030 (2021), arXiv:2010.00237 [hep-ph].

[19] R. Kleiss, W.J. Stirling, S.D. Ellis, *Comput. Phys. Commun.* **40**, 359 (1986).

[20] C.O. Rasmussen, T. Sjöstrand, *J. High Energy Phys.* **2016**, 142 (2016), arXiv:1512.05525 [hep-ph].